Patch transfer function as a tool to couple linear acoustic problems

Morvan Ouisse, Laurent Maxit, C. Cacciolati, Jean-Louis Guyader

Patch Transfer Functions as a tool to couple linear acoustic problems

Morvan OUISSE, Laurent MAXIT, Christian CACCIOLATI, Jean-Louis GUYADER

June 1, 2004

Abstract

A method to couple acoustic linear problems is presented in this paper. It allows one to consider several acoustic subsystems, coupled through surfaces divided in elementary areas called patches. These subsystems have to be studied independently with any available method, in order to build a database of transfer functions called Patch Transfer Functions, which are defined using mean values on patches, and rigid boundary conditions on the coupling area. A final assembly, using continuity relations, leads to a very quick resolution of the problem. The basic equations are developed, and the acoustic behavior of a cavity separated in two parts is presented, in order to show the ability of the method to study a strong-coupling case. Optimal meshing size of the coupling area is then discussed, some comparisons with experiments are shown, and finally a complex automotive industrial case is presented.

1 Introduction

Numerical modeling of acoustic behavior of industrial structures is still an open question. In the low and mid frequency domain, among many available methods, FEM [1] is a powerful approach for finite domains, while BEM [2] is suitable for infinite domains. In some cases, only one of these approaches is required to obtain the solution of a given problem, but sometimes, it is useful to decompose the domain in subdomains, and for each one, a given approach is appropriate, BEM, FEM or even analytical methods. Coupling these method directly [3] induces difficulties for large problems, since symmetry and sparsity properties of original formulations are lost because of the junction conditions. Many methods have been suggested to get rid of this problem, which are often based on separate resolution of the problems in each sub domain, with iterations on coupling

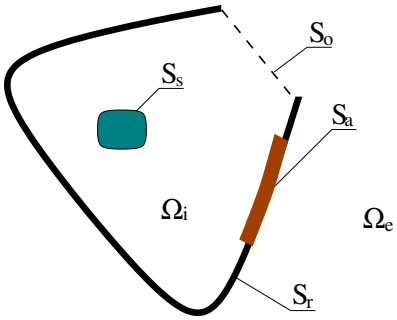

Figure 1: Example of basic acoustic problem

conditions until reaching convergence [4] [5], but the required iterations result in large calculation cost.

Using results of uncoupled structures to perform the response of the coupled one is a common thing in structural and acoustic analyses, using model reductions and substructuring [6]-[8], or impedance and mobility concepts [9], [10]. For structural-acoustic systems, weak coupling has been studied using modal impedances [11], and for purely acoustics problems, a point to point coupling between subdomains has been developed for structures like pipes or ducts [12]. The purpose of this paper is to describe a method for the analysis of acoustic domains coupled through a surface, which is a hole, divided in elements called patches. This approach is based on impedances evaluations between patches, sources, microphones and absorbing materials. Some validations on an academic case have been presented in reference [13]. These transfer functions called Patch Transfer Functions (PTF), are close to the ones called Acoustic Transfer Vectors (ATV) [14], which are typically used to reduce computational times for multi load cases studies. ATV approach has advantages in particular situations compared with some other methods [15], and have been improved to study industrial cases [16], [17], nevertheless they do not permit by themselves to couple two subdomains through a surface.

2 Patch Transfer Functions

2.1 Basic equations

The basic acoustic system considered here is described on figure 1, corresponding to sound radiation of a vibrating surface S_s (on which a harmonic normal velocity $\overline{V_n}$ is prescribed) in an "internal" volume Ω_i. This volume is closed by a surface $S_i = S_r \cup S_a \cup S_o$, including a rigid area S_r, some absorbing materials (characterized with acoustic impedance Z_a) placed on S_a, and an opening on

an area S_o to the "external" volume Ω_e. The acoustic pressure $p(M)e^{j\omega t}$ at point M, generated by the vibrating body is governed by the following equations: the internal problem 1, the external problem 2, coupled through continuity conditions 3.

$$\left\{\begin{array}{l} -\Delta p - k^2 p = 0 \ \forall M \in \Omega_i \\ \frac{\partial p}{\partial n} = -j\rho\omega\overline{V_n} \ \forall M \in S_s \\ \frac{\partial p}{\partial n} = 0 \ \forall M \in S_r \\ p = -Z_a \frac{1}{j\rho\omega}\frac{\partial p}{\partial n} \ \forall M \in S_a \end{array}\right. , \tag{1}$$

in which $k = \omega/c$ is the wave number,

$$\left\{\begin{array}{l} -\Delta p - k^2 p = 0 \ \forall M \in \Omega_e \\ \frac{\partial p}{\partial n} = 0 \ \forall M \in S_r \\ r\left(\frac{\partial p}{\partial r} + jkp\right) \to 0 \ as \ r \to \infty \end{array}\right. , \tag{2}$$

where the Sommerfeld conditions are taken into account, corresponding to free acoustic field (but of course any other conditions are admissible),

$$\left\{\begin{array}{l} p_i = p_e \ \forall M \in S_o \\ \frac{1}{j\rho\omega}\frac{\partial p_i}{\partial n_i} = -\frac{1}{j\rho\omega}\frac{\partial p_e}{\partial n_e} \ \forall M \in S_o \end{array}\right. , \tag{3}$$

in which the i subscript corresponds to internal values while e is used for external ones, with $n_i = -n_e$.

The method which is described here can also be applied to the coupling of two finite problems described as problem 1 or two semi-infinite problems, or even multi coupling of internal and external domains. The formulation of the proposed approach is presented on the previous equations.

2.2 Domain decomposition

In order to solve the coupled problem, the acoustic problem has to be decomposed in two subdomains, linked through the open area S_o which is divided in N_p surface elements called patches. This approach allows one to consider two uncoupled systems and to join them with few calculations. The optimal size of the mesh will be discussed in section 3.3. The basic idea is to estimate transfer functions between patches like explained here.

2.2.1 Internal problem

For each patch P of the N_p ones, the internal sub problem 4 has to be solved. The open area S_o where external and internal acoustic fields must be coupled, and the absorbing area S_a are here replaced by rigid walls for all patches except patch P on which a unit normal velocity is applied:

$$\begin{cases} -\Delta p - k^2 p = 0 \ \forall M \in \Omega_i \\ \frac{\partial p}{\partial n} = -j\rho\omega \ \forall M \in S_P \\ \frac{\partial p}{\partial n} = 0 \ \forall M \in S_i \setminus S_P \end{cases} . \tag{4}$$

The objective of this step is to calculate the Patch Transfer Functions (PTF) between excited patch P and rigid patch Q, defined as the ratio between the mean pressure on patch Q and the mean normal velocity on patch P (which has a unit value):

$$Z_{QP}^{int} = \frac{\langle p \rangle_Q}{\langle V_n \rangle_P} = \langle p \rangle_Q \ , \tag{5}$$

in which $\langle \bullet \rangle$ denotes the mean value: $\langle g \rangle_P = \frac{1}{S_p} \int_{S_P} g(M) dS$, and $V_n(M)$ is the normal velocity. This condensation of values on surfaces ensures convergence of the acoustic formulation, in particular on the excited patch: the consideration of coupling points instead of areas would involve a non-defined pressure at excitation point. The modal analysis of the cavity is used into a Green's function approach to built the PTF values, like indicated on appendix A. The resolution of the internal problem corresponds to the response of the whole rigid cavity to a unit velocity imposed on patch P. Then, a full $N_p \times N_p$ matrix of PTF has to be built for each frequency point. Assuming linearity of the phenomenon, these values will be used to calculate the response of the coupled system. As far as the internal measurement points that will be used as final output points are considered, they will be considered using patch-to-point transfer functions between excited patch P and listening point L:

$$z_{LP}^{int} = \frac{p(L)}{\langle V_n \rangle_P} = p(L) \ . \tag{6}$$

Then, if N_i listening points are defined inside, a $N_p \times N_i$ matrix is defined for each frequency point.

Finally, one has also to compute the uncoupled pressure corresponding to the response of the rigid cavity to the vibrating source surface S_s. One can divide this source area in N_s surface elements, in order to keep the same methodology: source PTF between patch R from the source

and rigid patch Q, defined as the ratio between the mean pressure on patch Q and the mean normal velocity on source patch R (which has a known value):

$$\widetilde{Z}_{QR}^{int} = \frac{\langle p \rangle_Q}{\langle \overline{V_n} \rangle_R} \ . \tag{7}$$

The associated patch to point transfer function from excitation patch R to listening point L is:

$$\widetilde{z}_{LR}^{int} = \frac{p(L)}{\langle \overline{V_n} \rangle_R} \ . \tag{8}$$

2.2.2 External problem

The methodology for the external problem is similar to the one presented above: one has to compute the PTF corresponding to mean pressure on patch P resulting from unit normal velocity excitation on patch Q:

$$Z_{QP}^{ext} = \frac{\langle p \rangle_Q}{\langle V_n \rangle_P} = \langle p \rangle_Q \ \ , \tag{9}$$

and the patch-to-point transfer function between excited patch P and listening external point L:

$$z_{LP}^{ext} = \frac{p(L)}{\langle V_n \rangle_P} = p(L) \ . \tag{10}$$

In the present case, it is assumed that all sources are located in the cavity and not in the exterior domain, thus terms $\widetilde{Z}_{QR}^{ext}$ and $\widetilde{Z}_{LR}^{ext}$ do not exist. However the presented methodology can obviously take into account external sources in the same way.

2.2.3 Introducing absorbing materials

With the proposed approach, it is quite simple to consider some absorbing materials: they should be considered as particular acoustic subsystems. For example when locally reacting materials are used, one has a known "auto-PTF" which is the acoustic impedance of the material, and a null "cross-PTF". The absorbing area is divided in patches, which are included in the previously described methodology, with the following values of PTF between patches A of S_a and any patch P of the system:

$$Z^a_{AP} = \delta_{AP} Z_a \ , \tag{11}$$

in which $\delta_{AP} = 1$ if $A = P$, and $\delta_{AP} = 0$ otherwise.

Of course some PTF between absorbing patches and other patches or excitation and listening points are needed to build the coupled pressure field. These transfer functions depend on the geometry of the system, and they are evaluated in the same way as in parts 2.2.1 and 2.2.2. It is clear that the methodology can be applied for other configurations, but it is supposed here that according to the figure 1, all absorbing materials are located in the cavity. In this case, the analysis which has been described in section 2.2.1 has to take into account not only the coupling patches, but also the patches corresponding to absorbing materials locations, and the PTF defined in equations 5, 6, 7 and 8 have to be evaluated for the whole set of patches.

2.2.4 Coupling conditions

Using the linearity properties of the system, the pressures p_{int} and p_{ext} corresponding to the internal and external ones on all patches of the coupled system verify the relations 12 and 13. The mean pressure on patch Q associated to internal field is:

$$\langle p_{int} \rangle_Q = \sum_{R=1}^{N_s} \widetilde{Z}^{int}_{QR} \left\langle \overline{V_n} \right\rangle_R + \sum_{P=1}^{N_p} Z^{int}_{QP} \left\langle V_n^{int} \right\rangle_P \ , \tag{12}$$

while the mean pressure on patch Q associated to external field can be expressed as:

$$\langle p_{ext} \rangle_Q = \sum_{P=1}^{N_{cp}} Z^{ext}_{QP} \left\langle V_n^{ext} \right\rangle_P \ . \tag{13}$$

In these relations, $\left\langle \overline{V_n} \right\rangle_R$ are the known velocity source terms (supposed to be all located in the cavity), while $\langle p_{int} \rangle_Q$ and $\langle p_{ext} \rangle_Q$ are the unknown mean pressures on patches (called coupling pressures), $\left\langle V_n^{int} \right\rangle_P$ and $\langle V_n^{ext} \rangle_P$ are the unknown mean normal velocities on patch P, associated to internal and external fields, called coupling velocities. The internal pressure field is the sum of the contribution of the Ns sources and of the N_p patches, including N_{cp} coupling patches and N_a absorbing patches ($N_p = N_{cp} + N_a$). For a sake of simplicity, one will suppose that coupling patches are numbered 1 to N_{cp}, while absorbing patches correspond to numbers $N_{cp} + 1$ to N_p.

Coupling values are determined using continuity relations 3, expressed on mean values of pressure and velocities for each coupling patch:

$$\langle p_{int} \rangle_Q = \langle p_{ext} \rangle_Q \quad \forall Q = 1, ..., N_{cp} \ , \tag{14}$$

$$\left\langle V_n^{int} \right\rangle_Q = - \left\langle V_n^{ext} \right\rangle_Q \quad \forall Q = 1, ..., N_{cp} \ , \tag{15}$$

in which $1, ..., N_{cp}$ are the coupling patches. For the N_a patches corresponding to absorbing materials locations, the relation is:

$$\langle p_{int} \rangle_A = Z_a \left\langle V_n^{int} \right\rangle_A = \sum_{P=1}^{N_p} Z_{AP}^a \left\langle V_n^{int} \right\rangle_P \quad \forall A = N_{cp} + 1, ..., N_{cp} + N_a = N_p \ . \tag{16}$$

This leads to a $N_p \times N_p$ linear system, using $\left\langle V_n^{int} \right\rangle_P$ as main unknowns. The N_{cp} first equations are related to the coupling patches (from equations 14 and 15):

$$\sum_{P=1}^{N_p} \left(Z_{QP}^{int} + Z_{QP}^{ext} \right) \left\langle V_n^{int} \right\rangle_P = - \sum_{R=1}^{N_s} \widetilde{Z}_{QR}^{int} \left\langle \overline{V_n} \right\rangle_R \quad \forall Q = 1, ..., N_{cp} \ , \tag{17}$$

while the N_a last ones correspond to the absorbing patches:

$$\sum_{P=1}^{N_p} \left(Z_{AP}^{int} - Z_{AP}^a \right) \left\langle V_n^{int} \right\rangle_P = - \sum_{R=1}^{N_s} \widetilde{Z}_{AR}^{int} \left\langle \overline{V_n} \right\rangle_R \quad \forall A = N_{cp} + 1, ..., N_{cp} + N_a = N_p \ . \tag{18}$$

The linear system which has to be solved (equations 17 and 18) is a full one, but its size is small. Its inversion leads to the coupling velocities values, that can be used in a post-processing phase in equations 12 and 13 to calculate averaged patch pressure on the coupling surface, and pressure at internal and external listening points with equations 19 and 20:

$$p^{int}(L) = \sum_{R=1}^{N_s} \widetilde{z}_{LR} \left\langle \overline{V_n} \right\rangle_R + \sum_{P=1}^{N_p} z_{LP}^{int} \left\langle V_n^{int} \right\rangle_P \ , \tag{19}$$

$$p^{ext}(L) = - \sum_{P=1}^{N_{cp}} z_{LP}^{ext} \left\langle V_n^{int} \right\rangle_P \ . \tag{20}$$

The expressions which are detailed here are valid for internal sources and internal absorbing materials. If this is not the case, in particular if some absorbing materials are also located in the external medium, one has two possibilities: the first issue is to change the definition of coupling area, in order to have a larger "cavity" which includes all absorbing materials. In this situation,

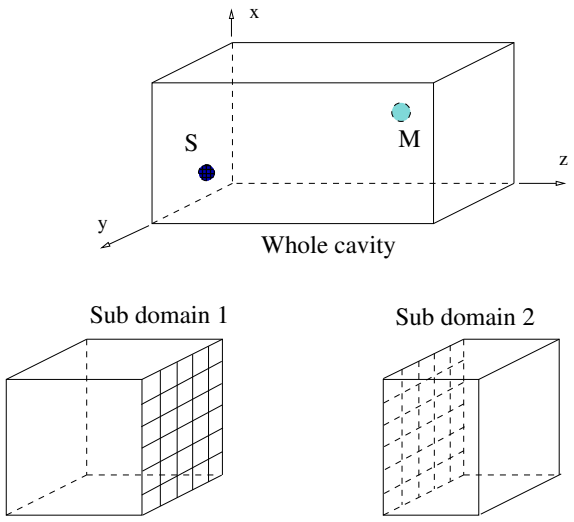

Figure 2: Rigid walled cavity

the above equations are still valid. The second approach needs a formulation of the problem with absorbing materials in the external domain, which is very close to the previous one, except that one can no longer use $\langle V_n^{int} \rangle_P$ as main unknowns in the final system: in this case the easiest way to proceed is to numerically solve the $2N_p \times 2N_p$ system which is directly obtained considering the coupling conditions and absorbing relations, using both normal velocities and pressure as unknowns.

3 Strong coupling application

In order to demonstrate the ability of the method to study cavities with strong coupling, the box described on figure 2 is considered here. It is a rigid box of size $0.7 \times 0.4 \times 1.2\ m^3$, filled with air ($\rho = 1.23\ kg.m^{-3}$; $c = 345\ m.s^{-2}$; $\eta_i = 10^{-2}$), including a point source placed at (0.2, 0.1, 0.1) and a microphone at (0.1, 1, 0.5). Such a cavity can be studied using analytical eigen modes. For the PTF method application, it has been decomposed in two sub domains named 1 (with a length of 0.8 m) and 2 (with a length of 0.4 m), and the coupling surface has been divided in patches.

3.1 PTF calculation with modes of rectangular sub cavities

Eigen modes of each rigid cavity can be obtained analytically: if the size of the box is $L_x \times L_y \times L_z$, the eigenfrequency corresponding to order $m \times n \times q$ of the box are:

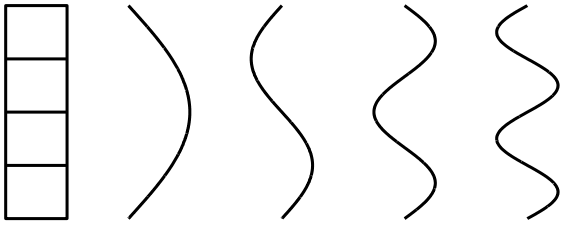

Figure 3: 4 patches and 4 modes

$$f_{nmq} = \frac{c}{2\pi}\sqrt{\left(\frac{m\pi x}{L_x}\right)^2 + \left(\frac{n\pi y}{L_y}\right)^2 + \left(\frac{q\pi z}{L_z}\right)^2}\,, \tag{21}$$

in which $L_x \times L_y \times L_z$ is the size of the box, and c the sound velocity. The corresponding eigen mode is:

$$\phi_{nmq}(x,y,z) = \cos\frac{m\pi x}{L_x}\,\cos\frac{n\pi y}{L_y}\,\cos\frac{q\pi z}{L_z}\,. \tag{22}$$

Then, the PTF of each uncoupled box are evaluated according to appendix A.

3.2 Choice of the number of modes

To insure non singular matrix when using PTF approach from modal expansion for cavity response, it has been seen that the number of modes to be taken into account is related to the number of patches which have been chosen to divide the coupling area. In order to describe this rule, it is useful to consider the figure 3, which is related to a mono dimensional visualization: four patches are presented, corresponding to a given mesh of the line. To solve the problem, coupling velocities on the four patches must be calculated, corresponding to four degrees of freedom for the problem to solve. In order to be able to reach these four degrees of freedom, one has to consider at least the first four modes (which are plotted on figure 3), otherwise some relationships between patches velocities exist, and the matrix associated to the resolution of the problem will be singular.

More modes could be used, corresponding to an ability to reach higher frequencies, but in this particular case, four modes should be the minimum. As a general rule for this mono dimensional problem, the number of modes used to calculate PTF has to be greater or equal to the patch number.

In the case of a bi dimensional coupling, which corresponds to the one proposed in this work, the same argument is valid, and the mode order of each direction should be larger than the corresponding number of patches to avoid numerical problems. This consideration is only related

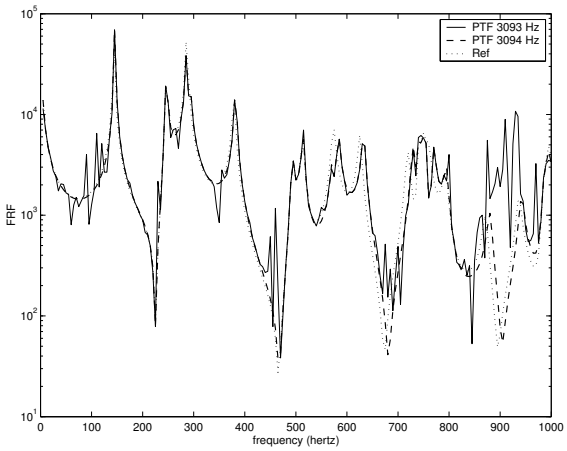

Figure 4: Influence of the number of modes on matrix conditioning.

to the singularity of the matrix, but not to the convergence of the method, that will be studied in the next part. In order to illustrate this phenomenon, one can consider a 10 by 6 patches division of the coupling area. Local mode of order (9,5,0) of cavity 2 (which is the smaller one), corresponding to the limit described above since one has to take into account the 0th order modes, has a resonant frequency of 3093.3 Hz. Using PTF approach with all modes up to 3093 Hz leads to badly conditioned matrices: the mean conditioning number on the frequency range up to 1000 Hz is 8×10^{16}, while using 3094 Hz as the limit, it is reduced to 2×10^4 due to the fact that the mode (9,5,0) is included in the analysis.

The figure 4 shows the results of the three calculations, including the reference one defined by the analytical modal analysis of the whole cavity. One can clearly see the instability of the results associated to ill conditioned matrix specially around 900 Hz.

However, one should note that this problem is related to the fact that the chosen coupling area is a plane one: changing modal order of z-axis has no influence on the conditioning of the problem. But for more complex cases, with curved coupling areas, each mode could be able to provide an additional degree of freedom: the problem of ill-conditioning would be less severe.

3.3 Convergence of the method

The box described on figure 2 is used here to study the convergence of the method with an increasing number of patches. The coupling area is divided in n_x by n_y patches like indicated on table 1, corresponding to patches lengths l_x and l_y. The convergence study is performed using modes up to 20th order in the three directions, for each cavity. So, the first missing frequency for the whole cavity is the (20,0,0) order, corresponding to 2875 Hz. The higher mode (19,19,19) has

n_x	1	3	5	7	10
n_y	1	2	3	4	6
$l_x\,(m)$	0.70	0.23	0.14	0.10	0.07
$l_y\,(m)$	0.40	0.20	0.13	0.10	0.067

Table 1: Coupling surface meshing size

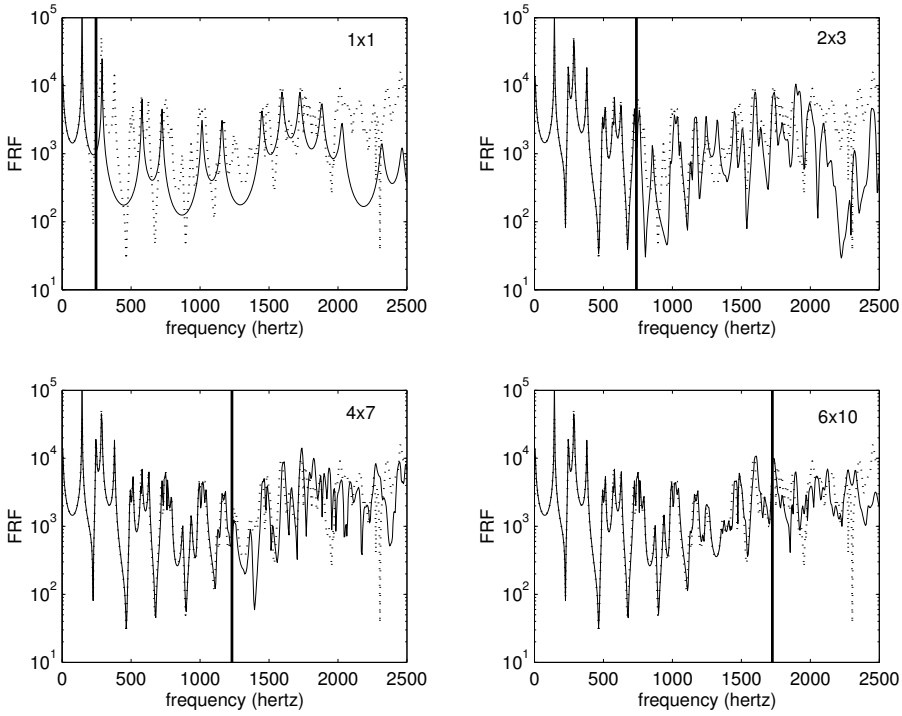

Figure 5: Convergence of pressure versus number of patches. Dotted line: reference calculation. The vertical line indicates the $\lambda/2$ limit.

a frequency of 9824 Hz.

The figure 5 shows the reference calculation, which is the analytical modal analysis of the whole cavity, with no use of PTF approach (in dotted lines), and the results of the PTF method using 1×1, 2×3, 4×7 and 6×10 patches. On theses plots, the frequency corresponding to the half-wavelength is indicated. From these results, it appears that there is a practical criterion for the PTF approach: the size of the patches should be smaller than the half-wavelength in order to obtain good results.

The figure 6 shows more precisely the convergence properties, by giving for two specific frequencies (500 and 1000 Hz), the pressure error at listening points, which is defined as:

$$e_{FRF} = |10 \log FRF_{ref} - 10 \log FRF_{PTF}| \ , \tag{23}$$

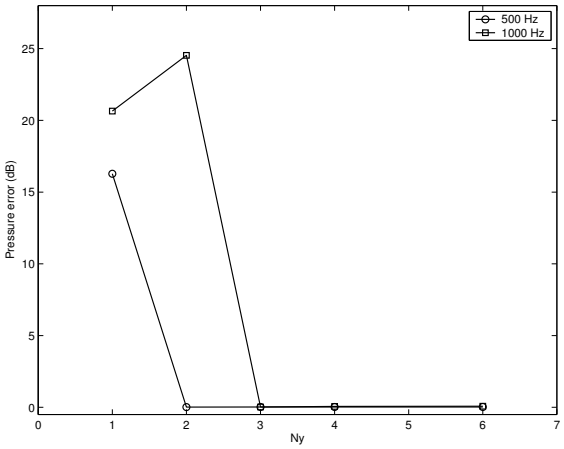

Figure 6: Pressure error at listening point versus number of patches along y axis.

in which the FRF are the transfer functions between excitation and listening point. The convergence is reached for 2×3 patches at 500 Hz and for 3×5 patches at 1000 Hz.

3.4 Conclusions on strong-coupling case

The validation of the method has been done on a strong-coupling case, and convergence rules have been derived. One can note that some comparisons with experiments, including use of absorbing materials, have been presented in [13].

4 Numerical and experimental validations on a complex structure

4.1 Description of the structure

In order to validate the methodology for automotive application, a complex structure has been designed and built by Rieter. It is presented on figure 7: this box has its lateral sides made of wood, on the upper part of it, the hood of a car has been placed, and on the bottom an undershield closes the cavity. On this part, a hole allows the sound to be radiated outside of the box. Some absorbing materials are used and placed in the cavity.

A loudspeaker is located inside the box, while some microphones are placed both inside and outside of it. The box is placed at 20 cm height, in order to have reflections on the ground: the objective was to be relatively close to the real Pass-By Noise problem.

For the application of the PTF method, the coupling patches have been defined in a very

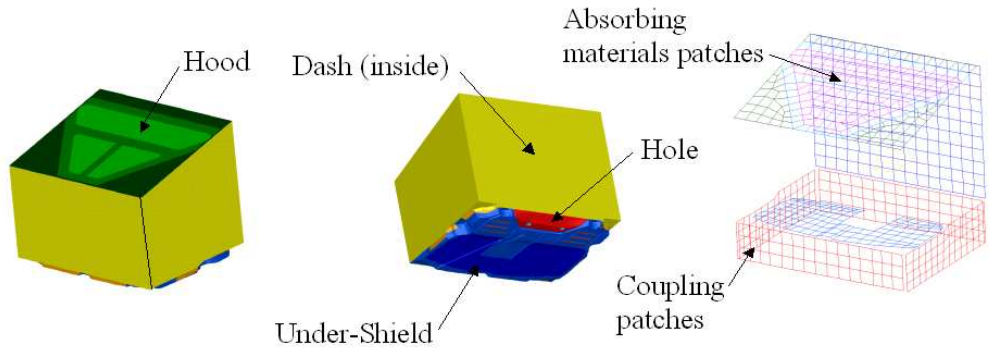

Figure 7: Description of the "Ground-Up Box" structure.

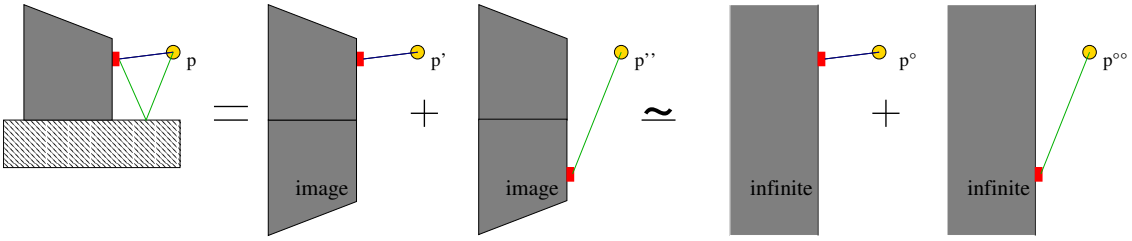

Figure 8: Image source theory illustration and Rayleigh simplified approach.

specific way, in order to use a simplified approach for the external domain, which is described in the next section.

4.2 Simplified Rayleigh approach

The complexity of the structure, associated to the need of mid frequency results (up to 2.5 kHz) can involve a prohibitive calculation cost for the external medium, even if the full coupled problem is not considered. In order to reduce calculation time, a simplified approach, based on Rayleigh integral has been used for the external problem. The choice of the patches definition and the use of a reflecting ground have been done in order to be as close as possible to Rayleigh's hypothesis: the Rayleigh integral allows one to know the pressure field radiated by a plane surface vibrating on a baffle. Calculations of PTF are then performed considering that the current patch (on which a unit velocity is imposed) vibrates on a given rigid plane: pressures can be evaluated only in a half-space, and other points are supposed to be silent. This is illustrated on figure 8: the pressure p radiated by a patch to a microphone location is the sum of the pressures p' and p'', which can be approximated by p° and $p^{\circ\circ}$ using infinite planes if the coupling patches are vertical. Another simplified approach could have been to consider a single layer potential methodology, or of course any BEM based method.

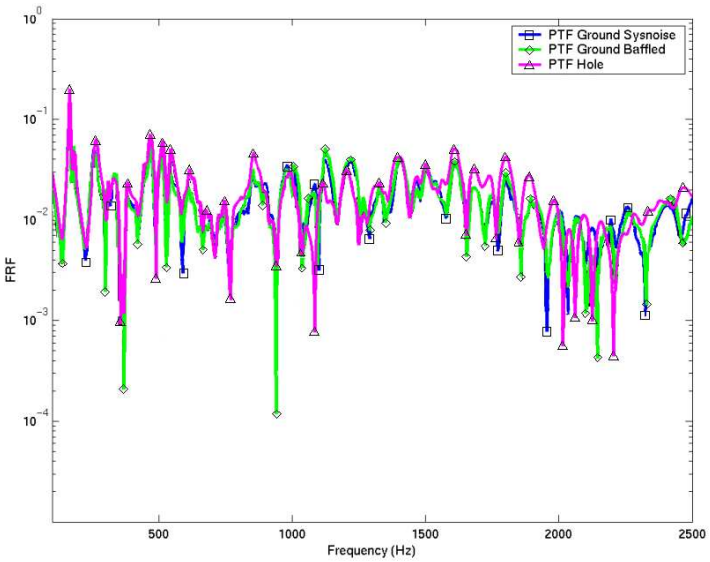

Figure 9: Comparisons between calculation techniques

4.3 Validation of the simplified approach

This simplified approach has been used for the analysis of the "Ground-Up Box", and the corresponding coupling patches are vertical, so the cavity includes the air which is located between the ground and the box, like indicated on figure 7. In order to measure the differences between the proposed simplified approach, three numerical tests have been performed. The two first ones are related to a choice of patches going from the box to the ground. The first one, called "PTF Ground Sysnoise", uses Sysnoise BEM to calculate the PTF, while the second one, called "PTF Ground baffled" uses the Rayleigh simplified approach, as described on figure 8. The third one is related to the standard mesh of the hole as coupling area: in this case it is impossible to apply the Rayleigh integral, because of the location of the ground. So a BEM approach has been used for this case. The results are presented in term of pressure over pressure FRF, between a microphone located outside the box, and another one located in the box.

It can be observed on this figure that the two PTF Ground calculations give very similar results, which are also quite close to the ones obtained using the hole as coupling area: in this case the simplified approach gives very satisfactory results, since the associated calculation time is very small compared to the one required for the BEM analysis.

These results have also been compared to experiments, like shown on figure 10. The two plots correspond to relative pressures at two listening points, one located close to the box, and the other one in the far field (several meters from the box). It can be observed that the differences

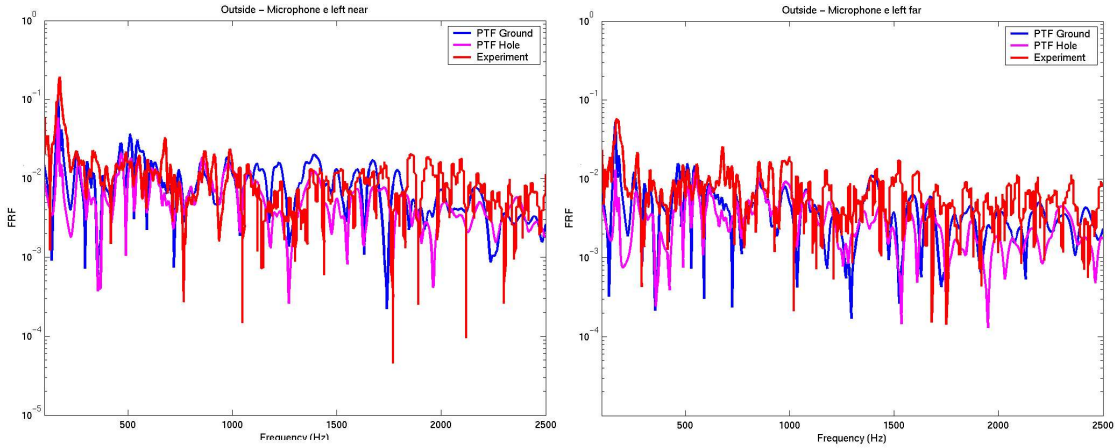

Figure 10: Comparisons between meshing methodologies and experiments.

between the two meshing methodologies is small compared to the difference between experiments and calculations. So the simplified Rayleigh approach can give very satisfactory results, providing that the meshing stage is done in order to be as close as possible to the Rayleigh hypotheses.

5 Automotive application

5.1 Description of the structure

In this section the ability of the method to be used on complex industrial cases is shown. The objective is to calculate the noise radiated through openings of engine cavity of an Alfa 156 car. The engine cavity has been modeled using acoustic FE, taking into account engine and all internal components of the engine cavity. The effects of the ground, supposed perfectly rigid, are taken into account using the image sources theory. The opening areas between the internal problem and the external ones are the holes located on the front of the car, and the surface defined by vertical areas going from the car body to the ground, like shown on figure 11. This particular definition of coupling areas corresponds to the simplified Rayleigh approach which has been described above.

Some absorbing materials are located in the engine cavity, they are considered as particular subsystems, like described in section 2.2.3. The coupling and absorbing areas are divided in patches, shown on figure 12, using the half-wavelength criterion to go up to 2500 Hz.

The Patch Transfer Functions of the internal cavity are evaluated using Green's function with modal analysis done with Nastran FE code, according to the appendix A, while the PTF of the external domain are calculated with the Rayleigh simplified approach.

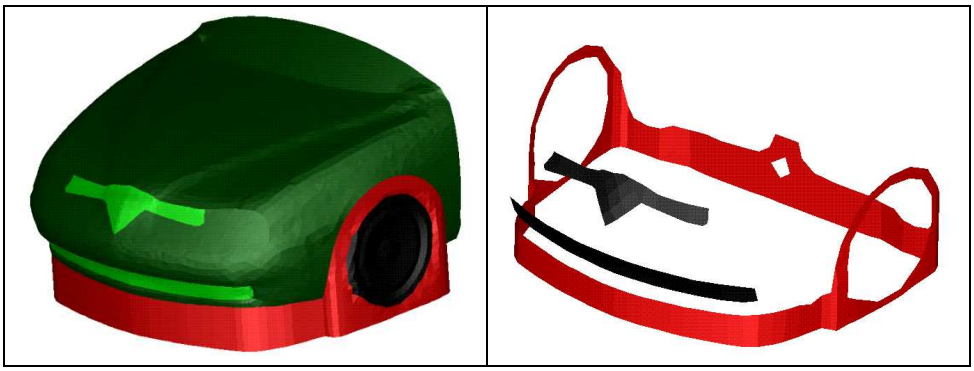

Figure 11: Front part of Alfa 156 and coupling areas for PTF application.

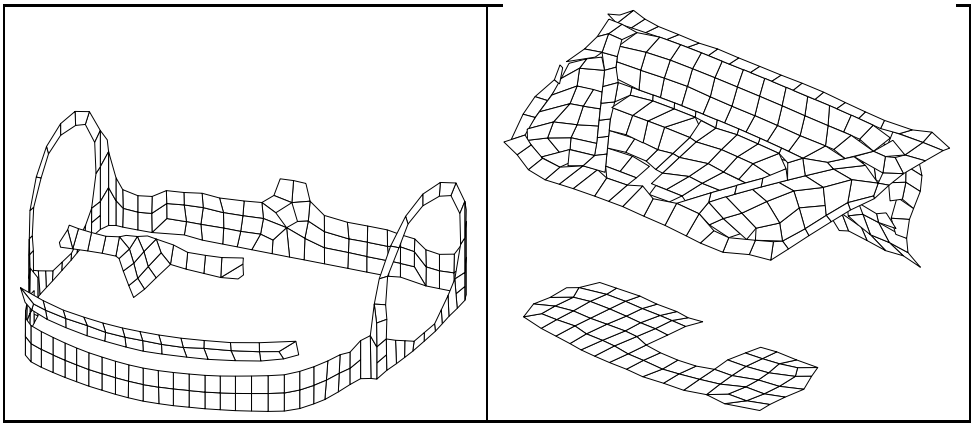

Figure 12: Patches definition on a) coupling areas and b) absorbing areas.

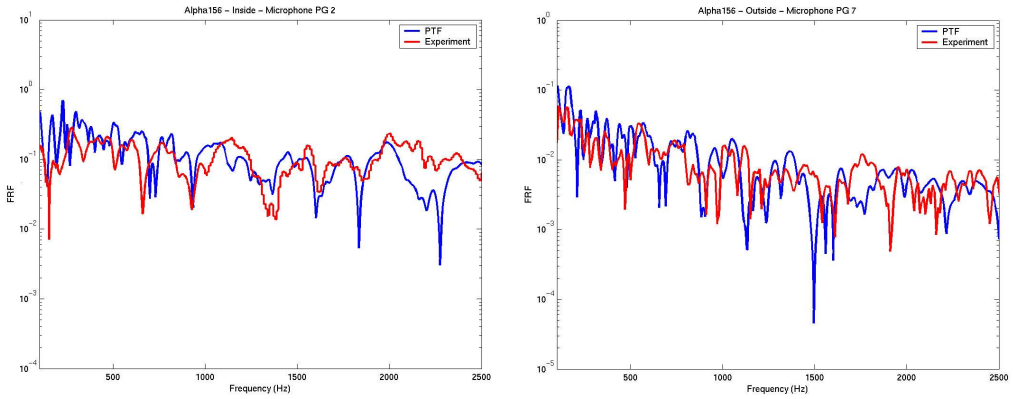

Figure 13: Comparisons between calculations and experiments, in terms of FRF, inside the cavity and at a pass-by microphone.

5.2 Results

5.2.1 Pressure transfer functions

Some measurements have been carried out on the real vehicle by CRF, in a semi-anechoic chamber. The excitation in this case is a point source, corresponding to a loudspeaker in the engine cavity. Absorbing materials have been used to cover the external part of the engine cavity in order to reduce the sound to be radiated by transparency. Some microphones are located both inside the engine cavity and in the external domain, in particular at Pass-By locations (7.5 meters on the side of the car).

The first comparisons with measurements, shown on figure 13, are related to transfer functions between inside and outside the cavity: a reference microphone has been chosen, and the plotted values are the relative pressures between interesting microphones and the reference one. It can be observed on this figure that the comparisons between calculated and measured pressures are quite reasonable, regarding the complexity of the structure.

5.2.2 Engine excitation

Some measurement with the real engine excitation have been also carried out by CRF, in a semi-anechoic chamber in rolling conditions (3rd gear, 3600 RpM). In this case, the noise sources which have been masked are the rolling noise (using slick tires) and the exhaust noise (using large silent muffler). Sources are defined using the so-called Monopole Substitution Technique [19], from measurement and FE model of the engine. 14 equivalent sources are located on the engine. The methodology used for the PTF approach is the same as above, and only a part of the PTF has

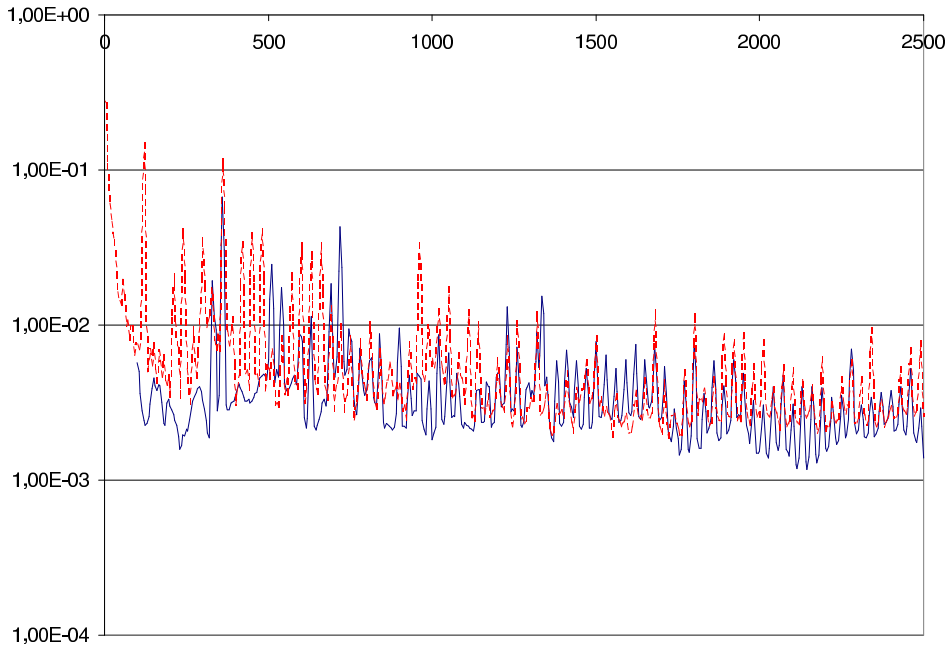

Figure 14: Comparison between experiments (dashed line) and simulations (continuous line) of radiated noise at a pass-by microphone location.

been calculated again, since many similarities exist between the two configurations. The only PTF that will differ from the previously evaluated ones are the sources to patches ones, and the uncoupled pressures. All other PTF keep the same values: in particular, the database of PTF for the external domain remains exactly the same.

The radiated pressure at a pass-by microphone location is shown on figure 14: experiments and numerical results are well correlated up to 2.5 kHz. The observed discrepancies are mainly due to the transparency of fenders of the car, which are not yet considered in the PTF approach.

6 Conclusion

The Patch Transfer Function approach allows one to solve a substructured acoustic problem, by considering uncoupled subsystems, which are analyzed separately with rigid boundary conditions. The coupling area has to be discretized in surface elements with a half-wavelength criterion, on which continuity relationships are verified on a mean sense. A database of PTF is built, defined

as acoustic impedance transfer functions between patches, excitation areas and listening points. A final assembly results in estimation of radiated pressure, with a very low calculation cost: the higher required cost corresponds to the PTF database building. A major advantage of the considered approach, compared to full coupled ones, is that effects of design or materials changes can be estimated very quickly: some changes in the shapes of a cavity require only the re-analysis of the modified cavity, which results in calculation time savings. Moreover, effects of changes of absorbing materials characteristics can be estimated with a very low calculation time, since these characteristics are introduced only at the final assembly stage, which consists in the inversion of a small linear system.

Acknowledgements

A part of this work has been carried out within the framework of the European research project VISPeR, GRD1-2000-25558. The authors would also like to thank CRF and RIETER who contributed to the industrial part of this work.

References

[1] O.C. Zienkiewicz, R.L. Taylor 1989 *The Finite Element Method, 1: Basic Formulation and Linear Problems.* McGraw Hill, 4th Edition, 648 pp.

[2] R.D. Ciskowski and C.A. Brebbia 1991 *Boundary element methods in acoustics.* Computational mechanics publications, Elsevier Applied Science.

[3] O.C. Zienkiewicz, D.W. Kelly and P. Bettess 1977 *International Journal for Numerical Methods in Engineering*, **11**, 355–375. The coupling of the finite element method and boundary solution procedures.

[4] D.M. Chiang and W.H. Chen 1999 *Journal of Vibration and Control*, **6**, 571–587. A combined FEM and BEM approach for sound radiation with finite flange.

[5] W.M. Elleithy and M. Tanaka 2003 *Computer Methods in Applied Mechanics and Engineering*, **192**, 2977–2992. Interface relaxation algorithms for BEM-BEM coupling and BEM-FEM coupling.

[6] R.J. Craig 1987 *International Journal of Analytical and Experimental Modal Analysis*, **2(2)**, 59–72. A review of time-domain and frequency domain component mode synthesis methods.

[7] M.A. Tournour, N. Atalla, O. Chiello and F. Sgard 2001 *Computers and Structures*, **79**, 1861–1876. Validation, performance, convergence and application of free interface component mode synthesis.

[8] G. Kergourlay, E. Balmès and D. Clouteau, 1998 *Proceedings of International Seminar on Modal Analysis ISMA 25, Leuven, Belgium.* Model reduction for efficient FEM/BEM coupling.

[9] S. Rubin 1967 *Journal of the Acoustical Society of America*, **41(5)**, 1171–1179. Mechanical immittance- and transmission-matrix concepts.

[10] G.J. O'Hara 1967 *Journal of the Acoustical Society of America*, **41(5)**, 1180–1184. Mechanical impedance and mobility concepts.

[11] S.M. Kim 1999 *Journal of Sound and Vibration*, **223(1)**, 97–113. A compact matrix formulation using the impedance and mobility approach for the analysis of structural-acoustic systems.

[12] W. Zhou and J. Kim 1998 *Journal of Sound and Vibration*, **219(1)**, 89–103. Formulation of four poles of three-dimensional acoustic systems from pressure response functions with special attention to source modeling.

[13] L. Maxit, C. Cacciolati and J.L. Guyader 2002 *Proceedings of International Congress on Sound and Vibration ICSV9, Orlanda, United States.* Airborne noise prediction using patch acoustic impedance.

[14] LMS International 2003 Sysnoise Rev 5.6, User's Manual.

[15] O. von Estorff 2003 *Acta Acustica united with Acustica*, **89**, 1–13. Efforts to reduce computation time in numerical acoustics - an overview.

[16] L. Cremers, M. Tournour and C.F. McCulloch 2001 *Proceedings of Inter-Noise 2001, The Hague, The Netherlands.* Panel acoustic contribution analysis based on acoustic transfer vectors.

[17] O. von Estorff and O. Zaleski 2003 *Engineering Analysis with Boundary Elements*, in press. Efficient acoustic calculations by the BEM and frequency interpolated transfer functions.

[18] J.P. Coyette, C. Lecomte and J.L Migeot 1999 *Acta Acustica united with Acustica*, **85**, 371–377. Calculation of vibro-acoustic frequency response using a single frequency boundary element solution and a Padé expansion.

[19] F. Augusztinovicz, P. Sas, L. Cremers, R.M.J. Liebregts, M. Mantovani, C. Bertolini 1999 *Proceedings of ISMA 21, Leuven, Belgium.* Prediction of insertion loss of engine enclosures by indirect BEM calculations, combined with a substitution monopole source description technique.

A Modal approach for internal problem

A.1 Modal composition for internal solution

The internal problem described in section 2.2.1 can be solved using the modal basis of the rigid cavity. Denoting ϕ_i the pressure eigen modes and k_i the corresponding wave numbers, this modal basis verifies the relations:

$$\begin{cases} -\Delta\phi_i(M) - k_i^2\phi_i(M) = 0 \quad \forall i,\ \forall M \in \Omega_i \\ -\frac{1}{j\rho\omega}\frac{\partial\phi_i}{\partial n}(M) = 0 \quad \forall i,\ \forall M \in S_i \end{cases} . \tag{24}$$

The normalization of theses modes is such as $\int_{\Omega_i} \phi_m\phi_n d\Omega = \Lambda_m\delta_{mn}$. The solution of problem 4 can be found using the Green's function $G(M,Q)$ of the internal rigid problem:

$$\begin{cases} -\Delta_M G(M,Q) - k^2 G(M,Q) = \delta(M-Q) \quad \forall M \in \Omega_i \\ -\frac{1}{j\rho\omega}\frac{\partial G}{\partial n_M}(M,Q) = 0 \quad \forall M \in S_i \end{cases} . \tag{25}$$

This Green's function can be determined using the modal basis:

$$G(M,Q) = \sum_i g_i(Q)\phi_i(M) \ . \tag{26}$$

Using this decomposition in equation 25, pre-multiplied by ϕ_q and integrated on Ω_i, one obtain :

$$\int_{\Omega_i} \sum_i g_i(Q)\phi_q(M)\phi_i(M)(k_i^2 - k^2)d\Omega = \phi_q(Q) \ , \tag{27}$$

which leads to the expression of g_q:

$$g_q(Q) = \frac{\phi_q(Q)}{\Lambda_q(k_i^2 - k^2)} \ . \tag{28}$$

Finally the Green's function can be expressed with the modes of the rigid cavity:

$$G(M,Q) = \sum_i \frac{c^2}{\Lambda_i} \frac{\phi_i(M)\phi_i(Q)}{(\omega_i^2 - \omega^2)} \ . \tag{29}$$

Applying Green's theorem to problem 4 with no internal source leads to:

$$p(M) = \int_{S_i} \left(G(M,Q)\frac{\partial p}{\partial n}(Q) - p(Q)\frac{\partial G}{\partial n}(M,Q) \right) dS = -\int_{S_P} G(M,Q) j\omega\rho dV \ , \tag{30}$$

and the solution of problem 4 is:

$$p(M) = \sum_i j\omega \frac{\rho c^2}{\Lambda_i} S_P \left\langle \phi_i \right\rangle_P \frac{\phi_i(M)}{\omega^2 - \omega_i^2} \ . \tag{31}$$

A.2 PTF modal expressions

Using the previous expressions, one can deduce values of PTF defined in section 2.2.1. The source PTF 5 between patch R from the source and rigid patch Q, is:

$$Z_{QP}^{int} = \sum_i j\omega \frac{\rho c^2}{\Lambda_i} S_P \frac{\left\langle \phi_i \right\rangle_P \left\langle \phi_i \right\rangle_Q}{\omega^2 - \omega_i^2} \ . \tag{32}$$

The patch-to-point transfer functions 6 between excited patch P and listening point L is:

$$z_{LP}^{int} = \sum_i j\omega \frac{\rho c^2}{\Lambda_i} S_P \frac{\left\langle \phi_i \right\rangle_P \phi_i(L)}{\omega^2 - \omega_i^2} \ . \tag{33}$$

The source PTF 7 between patch R from the source and rigid patch Q, is:

$$\widetilde{Z}_{QR} = \sum_i j\omega \frac{\rho c^2}{\Lambda_i} \frac{S_R}{\left\langle \overline{V_n} \right\rangle_R} \frac{\left\langle \phi_i \right\rangle_R \left\langle \phi_i \right\rangle_Q}{\omega^2 - \omega_i^2} \ . \tag{34}$$

The patch to point transfer function 8 from excitation patch R to listening point L is:

$$\widetilde{z}_{LR} = \sum_i j\omega \frac{\rho c^2}{\Lambda_i} \frac{S_R}{\langle \overline{V_n} \rangle_R} \frac{\langle \phi_i \rangle_R \, \phi_i(L)}{\omega^2 - \omega_i^2} \ . \tag{35}$$

A.3 Air damping introduction

The modal composition presented above without losses induces problems at resonant frequencies. This is avoided using modal damping of fluid η_i, which induces a change in expression of denominators of equations 29 to 35: the term $\omega^2 - \omega_i^2$ has to be replaced by $\omega^2 - j\eta_i\omega_i\omega - \omega_i^2$.

List of Figures

List of Tables